Resonant Type MEMS Transducers Excited by Two Acoustic Emission Simulation Techniques

Didem Ozevin[a*], David W. Greve [b], Irving J. Oppenheim[c], Stephen Pessiki[a]
[a]Dept. of Civil and Environmental Engineering, Lehigh University, Bethlehem, PA 18015
[b]Dept. of Electrical and Computer Engineering, Carnegie Mellon University, Pittsburgh, PA 15213
[c]Dept. of Civil and Environmental Engineering, Carnegie Mellon University, Pittsburgh, PA 15213

ABSTRACT

Acoustic emission testing is a passive nondestructive testing technique used to identify the onset and characteristics of damage through the detection and analysis of transient stress waves. Successful detection and implementation of acoustic emission requires good coupling, high transducer sensitivity and ability to discriminate noise from real signals. We report here detection of simulated acoustic emission signals using a MEMS chip fabricated in the multi-user polysilicon surface micromachining (MUMPs) process. The chip includes 18 different transducers with 10 different resonant frequencies in the range of 100 kHz to 1 MHz. It was excited by two different source simulation techniques; pencil lead break and impact loading. The former simulation was accomplished by breaking 0.5 mm lead on the ceramic package. Four transducer outputs were collected simultaneously using a multi-channel oscilloscope. The impact loading was repeated for five different diameter ball bearings. Traditional acoustic emission waveform analysis methods were applied to both data sets to illustrate the identification of different source mechanisms. In addition, a sliding window Fourier transform was performed to differentiate frequencies in time-frequency-amplitude domain. The arrival and energy contents of each resonant frequency were investigated in time-magnitude plots. The advantages of the simultaneous excitation of resonant transducers on one chip are discussed and compared with broadband acoustic emission transducers.

Keywords: Acoustic emission, MEMS, pencil break, impact, sliding window Fourier transform.

1. INTRODUCTION

Acoustic emission (AE) testing is a passive nondestructive testing technique used to identify the onset and characteristics of damage through the detection and analysis of transient stress waves. Identification of the AE source from the characteristics of received signals is still a research issue, which depends in part on the characteristics of the transducer. We have previously reported fabrication of a MEMS chip in the multi-user polysilicon surface micromachining (MUMPs) process specifically for acoustic emission testing[1]. Here, we will report on the mechanical behavior and performance of these MEMS transducers when excited by two acoustic emission simulation techniques.

2. DESCRIPTION OF MEMS TRANSDUCERS

The chip includes 18 different transducers with 10 different resonant frequencies in the range of 100 kHz to 1 MHz. Figure 1 shows the chip layout and the characteristics of transducers on the chip. There are two mechanical configurations on the chip, referred to as the hexagonal plate design and the piston design, covering high frequencies and low frequencies, respectively. The hexagonal plate design makes diaphragm deflection under excitation. The piston design is similar to accelerometers and exhibits both out-of-plane rotational and translational rigid body motions. The first modal frequency values of piston type designs in Figure 1 correspond to rotational motion and the other modes correspond to translational motion.

[*] Contact author:dio2@lehigh.edu; 610-758-6966; 117 ATLSS Drive Lehigh University, Department of Civil and Environmental Engineering, Bethlehem, PA, 18015.

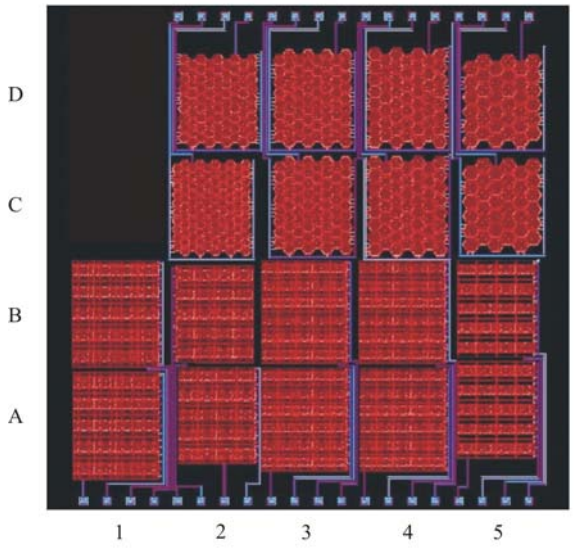

Type	Location	Resonant frequency (kHz)	C1(F)-static sensitivity (experiment results)
piston	A1	112-165	1.53E-14
	B1	112-165	1.14E-14
	A2	152-225	2.09E-15
	B2	152-225	2.22E-15
	A3	195-294	4.88E-15
	B3	195-294	4.77E-15
	A4	211-325	2.92E-15
	B4	211-325	3.01E-15
	A5	133-201	8.43E-15
	B5	133-201	7.24E-15
hexagon	C2	1065	5.33E-16
	D2	812	7.28E-16
	C3	660	1.38E-15
	D3	660	1.63E-15
	C4	482	3.04E-15
	D4	482	4.28E-15
	C5	362	4.93E-15
	D5	362	4.88E-15

Figure 1. MEMS chip layout and the characteristics of transducers

3. SIMULATION TECHNIQUES AND BLOCK DIAGRAMS

Short duration acoustic emission bursts resulting from mechanical deformation in a structure can be simulated by several methods: pencil lead break, glass capillary fracture, impact loading and the fracture of SiC grains[2]. In this research, two qualitatively different methods, impact loading with steel spheres and pencil lead break, were chosen as acoustic simulation methods. These methods were chosen because they are experimentally convenient and as well as repeatable. The first simulation was repeated for five different diameter ball bearings; 0.96 cm, 0.80 cm, 0.64 cm, 0.48 cm, 0.32 cm. The drop height was 14.50 cm. According to ASTM E976-00[3], breaking 0.5 mm 2H pencil lead on a structure creates an impulse signal that can be used to determine the reproducibility of acoustic emission tranducer response. The pencil lead break was accomplished by breaking 0.5 mm lead on the ceramic package. Four transducer outputs were collected simultaneously using a multi-channel oscilloscope. Experiments were repeated three times and average magnitudes were computed to determine the relative sensitivities of each transducer.

The MEMS chip with its package and four identical amplifiers were placed on a breadboard along with a custom-designed preamplifier using LM6171 high speed low power op-amps with 100 MHz gain-bandwidth product. Amplifiers had a voltage gain of 10 up to 2 MHz and an input resistance of 100 kohm. The MEMS chips were mounted in a ceramic package with an attached pumping port so that the ambient pressure could be varied. Ambient pressure has a substantial impact on the quality factor Q of the transducers through the pressure dependence of squeeze-film damping.

Figure 2 shows block diagrams for impact and pencil break excitations. Transducers were tested in a vacuum environment as shown in the block diagram. It was observed that squeeze film damping at atmospheric pressure was so high that vibration motion could not be observed. A Q factor for the lowest frequency design was estimated to be 0.26 based on lubrication theory[4]. For impact loading, experiments were repeated for the cases of (1) vacuum on-bias on; (2) vacuum on-bias off; (3) vacuum off-bias on; and (4) vacuum off-bias off in order to observe the vacuum effect. Comparison of (1) and (2) also allows us to verify that the signal is due to vibration of the transducer as the signal should disappear when the bias voltage is removed. A 1 MHz PZT (Krautkramer MSW-QC) transducer was attached to one of the channels for comparison of signal profiles during impact excitations. For the pencil lead break, the outputs of four transducers on the MEMS chip were collected simultaneously. 21 different sets of transducers were tested with the PZT transducer employed as the external trigger source.

(a)

(b)

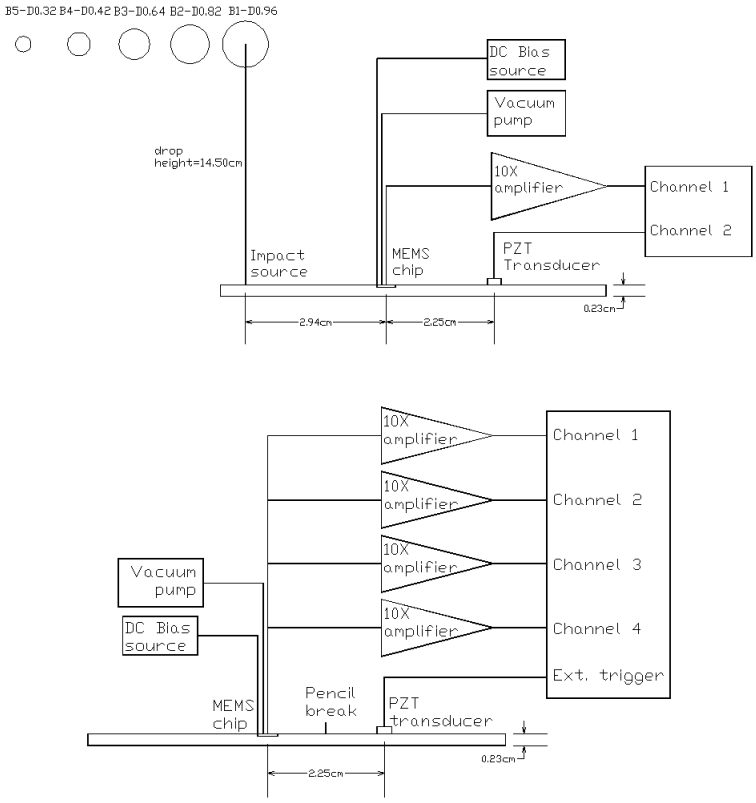

Figure 2. Block diagrams, (a) Impact loading, (b) Pencil break

4. ACOUSTIC EMISSION PARAMETERS

Acoustic emission waveforms carry information about the characteristics of source event. In the literature, AE parameters are defined in order to correlate the experimental results with the AE source event. Stephens and Pollock[5] have reviewed various emission parameters and their interpretations. Some important parameters were listed along with their interpretations in Table 1.

Table 1. Acoustic emission parameters and their information about the source event

Domain	Parameter	Information about the source event
Time domain variables	Rate	Rate of damage occurring
	Peak amplitude	Intensity of source event, orientation
	Relative arrival times	Source location
	Duration or count	Energy of source event
	Waveform	Structure of source event
	Energy	Energy of source event-damage type
Frequency domain variables	Frequency spectrum	Nature of source event
Time-frequency domain variables	Spectrogram	Energy distribution of source event through time
	The time variation of each frequency component	The intensities of source frequency components

5. INTERPRETATION OF EXPERIMENTAL RESULTS WITH TRADITIONAL PARAMETERS

5.1 Impact loading

As the thickness of the plate was not sufficiently large to prevent the return of reflected elastic waves to the contact point before the end of the impact, Hertz Impact Theory was not applicable. On the other hand, it is known that as the diameter of the ball bearing becomes smaller, frequency components of the input signal extend to higher frequencies while the amplitude of the input signal decreases[6]. As we will show below, low frequency designs resulted in larger responses to the ball bearing excitations.

Figure 3 demonstrates examples of hexagonal design and piston design output signals when the test structure was excited by impact loading. The first two columns show hexagonal design transients (column 1) along with PZT transducer transients which were collected simultaneously (column 2). The next two columns illustrate piston type design transients (column 3) and PZT transducer transient (column 4), also collected simultaneously. As we stated in Section 3, transducers were tested under four different atmospheric pressure and bias conditions. The first row shows the results at atmospheric pressure and with no bias voltage. The second and third rows were collected at atmospheric pressure and with the bias voltage on. The fourth row shows the case of vacuum and with no bias voltage. Finally, the last two rows are transients collected with vacuum and with the bias voltage on. 20V and 8V DC bias voltages were applied to hexagon designs and piston designs, respectively. The vacuum effect is more apparent for the piston design, which has resonant frequencies of 133 kHz and 201 kHz. Frequency domain analysis (not shown) demonstrates that the responses of devices under atmospheric pressure conditions contain only low frequency components. This is the reason that hexagon design responses in both atmospheric and vacuum conditions look similar, as hexagon designs cover frequencies higher than effective frequency range of impact loadings.

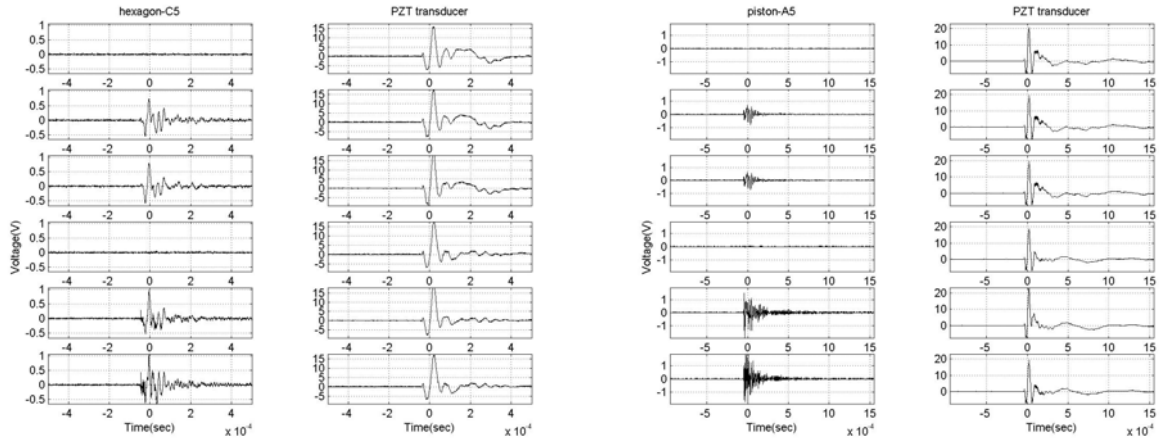

Figure 3. Output signals of (a) hexagon-C5 and (b) piston-A5 under ball#1

Figures 4 and 5 show two examples of hexagon designs and piston designs outputs when 200 kHz and 90 kHz high-pass filters were applied to hexagon designs and piston designs, respectively. When frequency amplitudes of each device under different diameter ball bearings were compared, the frequency content of the excitation signal and the intensity of the corresponding frequency can be identified.

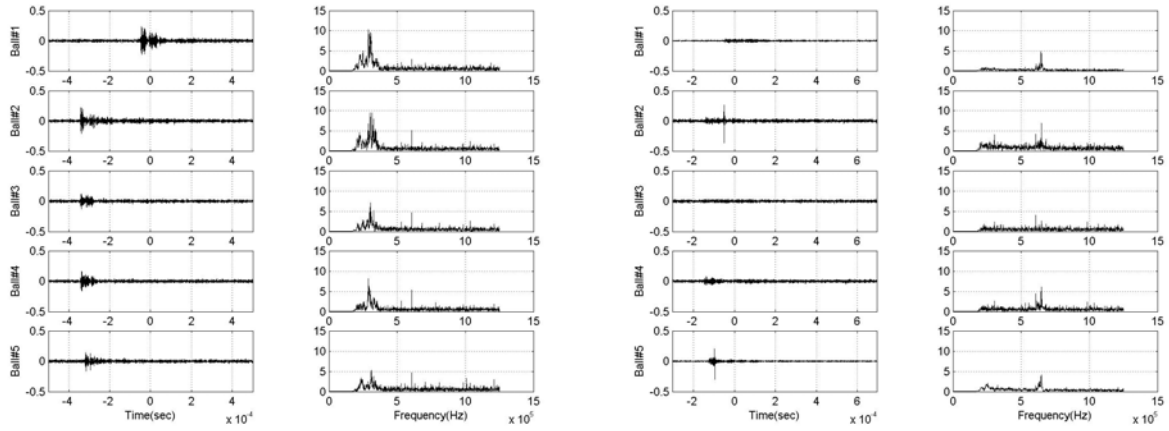

(a) (b)

Figure 4. Time domain outputs and frequency spectra of (a) hexagon-C5 and (b) hexagon-C3 when Vdc=20V under vacuum condition for five ball bearings with 200 kHz high-pass filter

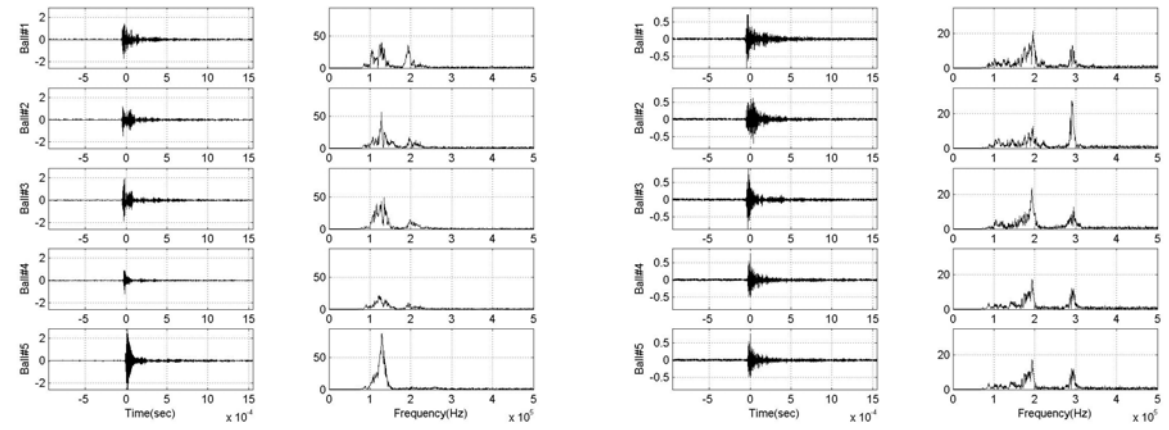

(a) (b)

Figure 5. Time domain outputs and frequency spectra of (a) piston-A5 and (b) piston-A3 when Vdc=8V under vacuum condition for five ball bearings with 90 kHz high-pass filter

5.2 Pencil lead break

As noted in the impact loading section, transducers were tested under four different conditions. In addition, four-channel data acquisition was performed during pencil break experiments as shown in the block diagram, Figure 2b. 21 different channel configurations were tested. Figures 6 and 7 show two examples of hexagon designs and piston designs tested under vacuum condition with the proper bias voltages. The same high-pass filters as in the impact loading analyses for hexagon designs and piston designs were applied to the collected signals.

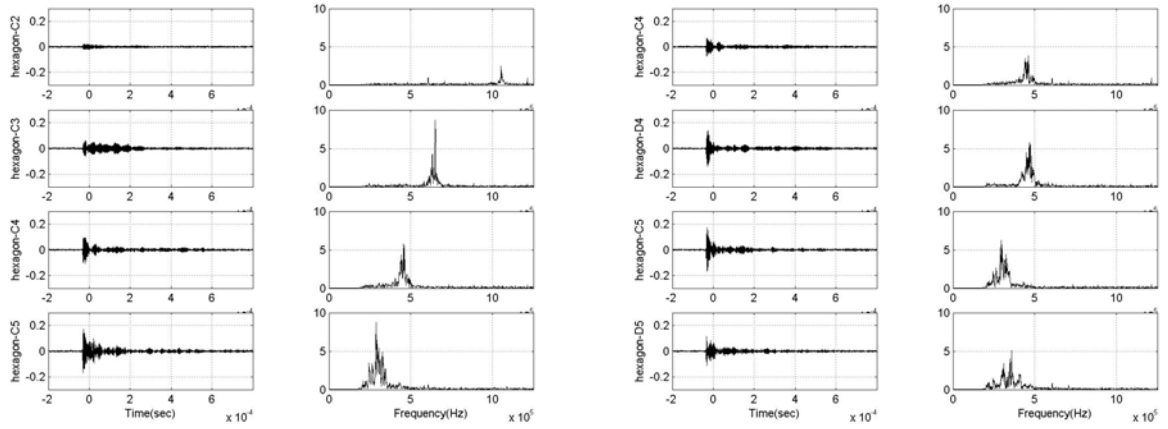

(a) (b)

Figure 6. Time domain outputs and frequency spectra of (a) transducer set of hexagons-C2-C3-C4-C5 and (b) transducer set of hexagons-C4-D4-C5-D5

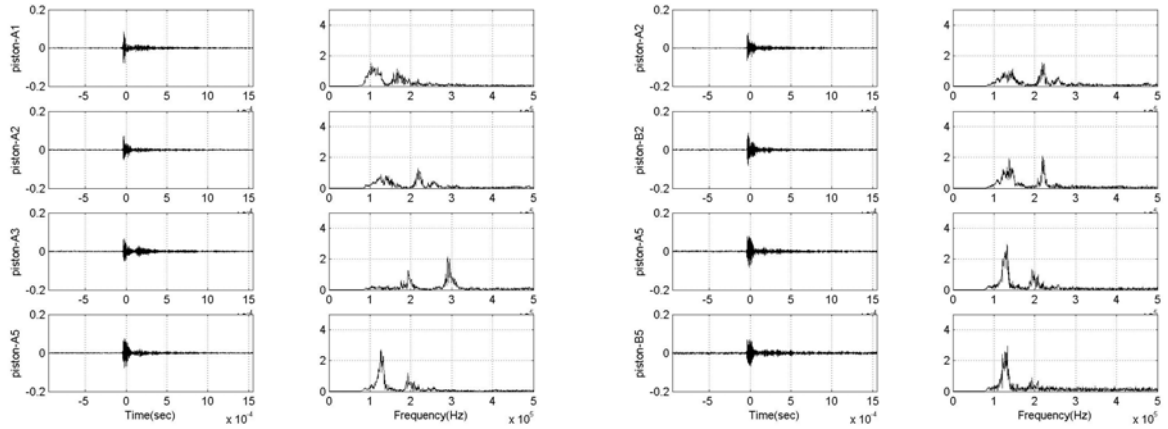

(a) (b)

Figure 7. Time domain outputs and frequency spectra of (a) transducer set of pistons-A1-A2-A3-A5 and (b) transducer set of pistons-A2-B2-A5-B5

Figure 8 shows the maximum signal amplitudes for the tested devices and their error bars after the data were filtered. It is known that pencil lead break provides a good approximation to impulse excitation, that is, it has a flat frequency spectrum in the range of interest[3]. This characteristic of input excitation makes it possible to compare the relative sensitivities of devices. Generally, we found that devices with the same designs have closely similar sensitivity, although in a few cases (for example A1 and B1 in Figure 8) this was not the case. We attribute this to variations in the surface micromachining process or possibly differences in the location of transducers on the chip.

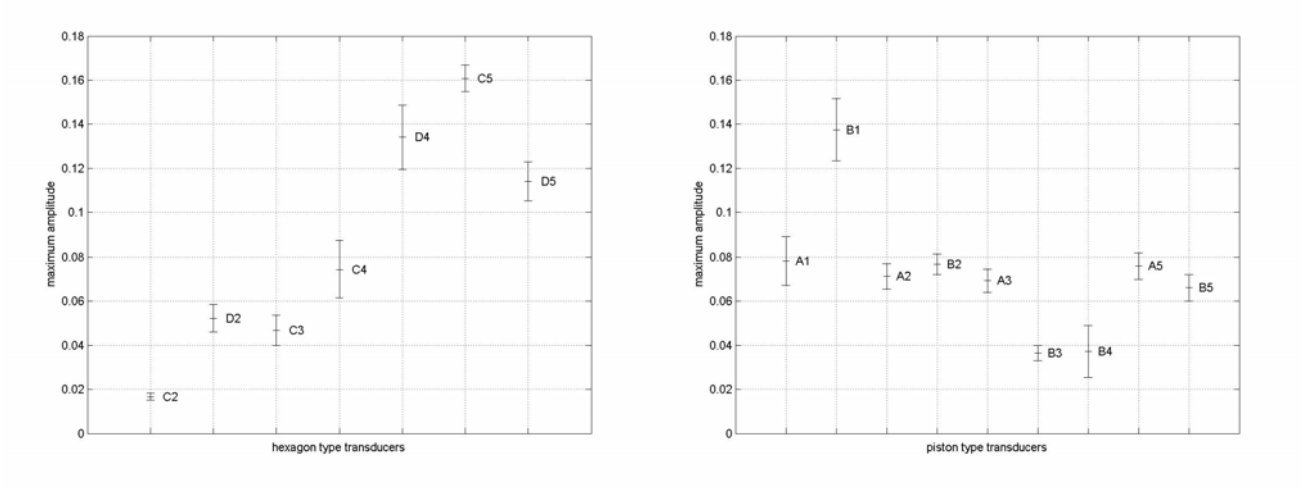

(a) (b)

Figure 8. Maximum amplitudes and error bars for (a) hexagon type transducers, (b) piston type transducers

5.3 Comparison of Impact and Pencil lead break experiments

A subroutine was written in Matlab in order to compute several conventional acoustic emission parameters, specifically, (1) the duration of the signal from the first threshold crossing to the last one, (2) minimum and maximum amplitudes, (3) energy computed by the area of signal during the duration of the event and (4) risetime computed by time difference from the first threshold crossing to time at the maximum amplitude. 12 mV was taken as the threshold level.

Variables that identify the characteristics of a source event were defined in Table 1. Hamstad and Sendeckyj[7] noted the change in the waveform due to the nature of transducer. They suggested using different parameters for broadband transducers and resonant type transducers. Resonant type transducers filter the input signal according to their transfer function; therefore waveforms cannot be used directly to relate to the source event. As MEMS transducers under high vacuum conditions show resonant behavior at particular frequencies, energy, duration and frequency contents of the signals were considered as the main parameters correlated to source events. Figures 4, 5, 6 and 7 demonstrate how intensities of different frequencies change with source type. Figure 9 shows the energy and duration variations of devices when pencil lead break and various impact loadings were used as the excitation sources. It is clear that the plots are different when the source type is changed. In Figure 10, duration and risetime were investigated. We conclude that risetime vs. duration cannot be used to classify the source characteristic.

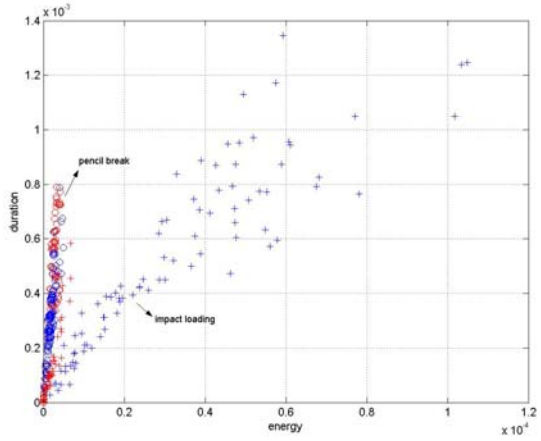

Figure 9. Energy-duration plots for impact experiments and pencil lead break experiments

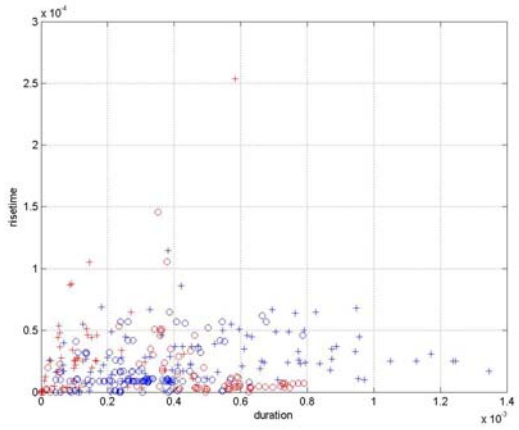

Figure 10. Duration-risetime plots for impact experiments and pencil lead break experiments

6. INTERPRETATION OF EXPERIMENTAL RESULTS WITH TIME-FREQUENCY ANALYSES

Time-frequency (TF) analysis of a signal is a method that extracts the time variation of each frequency component of a signal. There are several methods that have been suggested for determining the signal characteristics in TF domain. Short Time Fourier transform (STFT), Wagner-Ville Distribution[8] (WVD) and Wavelet Transform[9] (WT) are commonly used methods in the literature. While it is not possible to provide high resolution in both time and frequency by STFT, this method was used to calculate TF of the signals in this research, as high time-frequency resolution was not required. Better resolution would be desirable if the time of arrival varied significantly for different frequency components. However, as the experimental setup was small, the variation in arrival time is small and there is no need for high resolution. STFT splits the signal into overlapping sections and applies a window specified by a window parameter to each section. Then the Fourier transform of each section with data length of 2500 is computed to produce an estimate of the short-term frequency content of the signal. The transform equation is

$$F(\omega,b)=\frac{1}{2\pi}\int_{-\infty}^{+\infty} f(t)g(t-b)e^{-i\omega t}dt \tag{1}$$

where f(t) is the signal in the time domain, g(t-b) is the windowing function with b is a parameter characterizing the window width. We chose the Kaiser Window as the windowing function. The Kaiser Window has two parameters: the length of the signal to be windowed and a shape parameter β. By varying these two parameters, the window length and shape can be adjusted to trade side-lobe amplitude for main lobe width[10]. The parameters are chosen to adjust the resolution in order to obtain the best display of the signal behavior. In this research, we chose the length as 50 with overlapping 45 and shape parameter β as 4.

Figures 11 and 12 show spectrogram displays of two transducer sets of hexagons and pistons, which are given in Figures 6 and 7. The frequency content of the signals, the duration of a specific frequency and the signal bandwidth can be determined from these plots.

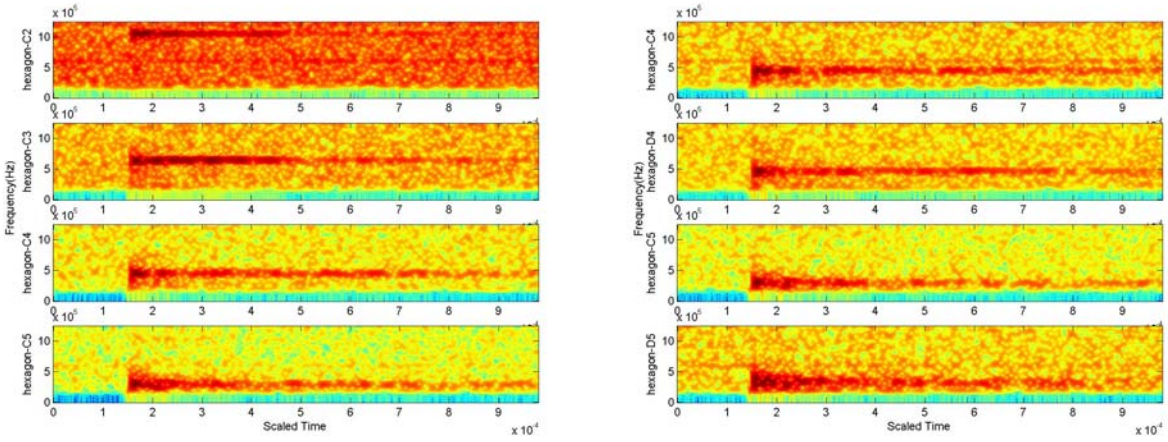

(a) (b)

Figure 11. Time-Frequency images of (a) transducer set of hexagons-C2-C3-C4-C5 and (b) transducer set of hexagons-C4-D4-C5-D5

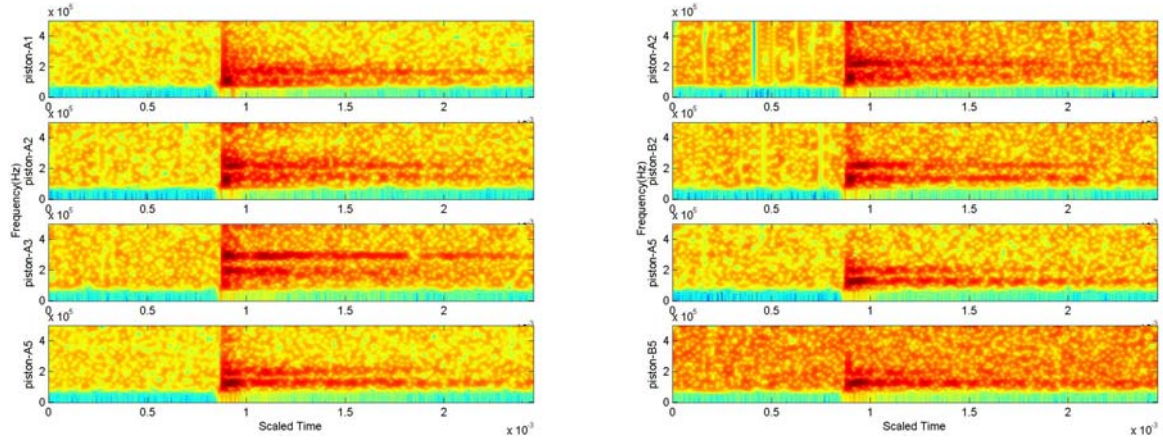

(a) (b)

Figure 12. Time-Frequency images of (a) transducer set of pistons-A1-A2-A3-A5 and (b) transducer set of pistons-A2-B2-A5-B5

The Fourier transform amplitude at a particular frequency, ω_n, as a function of time is given by

$$F_{abs}(b)\Big|_{\omega=\omega_n} = \left| \frac{1}{2\pi} \int_{-\infty}^{+\infty} f(t)g(t-b)e^{-i\omega_n t}dt \right| \tag{2}$$

where ω_n is the natural frequency of transducer. Figure 13 shows a plot of $F_{abs}(b)\Big|_{\omega=\omega_n}$ for hexagon type transducers used in the transducer set of hexagons-C2-C3-C4-C5. It is clear to see how intensities of different frequencies change through the duration of the event. In addition, it is known that each peak at the time-amplitude plots of a particular frequency with an enhanced time-frequency resolution corresponds to arrival of new waveform[9]. We can distinguish the arrivals of piston modes through time-FFT amplitude plots. Additionally, it becomes an advantage to collect multiple frequency-selective transducer outputs simultaneously to diminish the source location error as the number of arrival comparison possibilities increases.

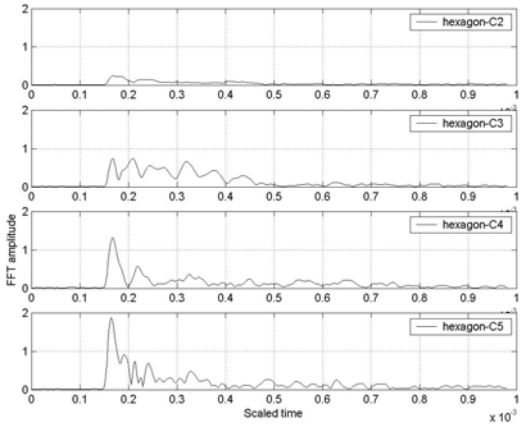

Figure 13. The time variation of each frequency component of the signals collected during the transducer set of hexagons-C2-C3-C4-C5 under pencil lead break

Here, we suggest that energy of entire waveform of a transducer and the energy content of its natural frequency ω_n, which can be computed by areas under Figure 13, should be proportional as we observe resonance waveforms at output signals. The same plots as shown in Figure 13 were determined for all transducer sets and the areas were computed. With some exceptions, values show a characteristic trend for each transducer. As demonstrated in Figure 14, energy values computed in the time domain and area values show the same trend for hexagon designs and piston designs for the same type of source event.

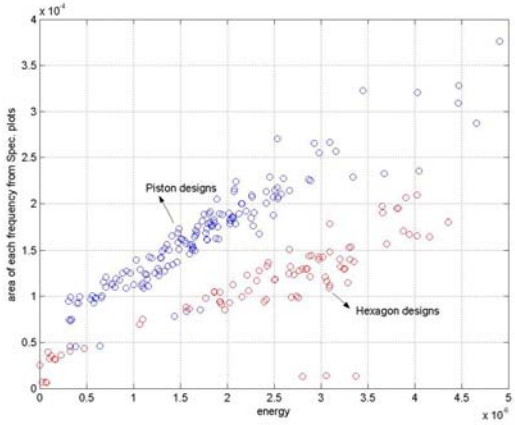

Figure 14. Energy of entire waveform and energy of each frequency component of the signals collected under pencil lead break

6. COMPARISON OF RESULTS WITH BROADBAND ACOUSTIC EMISSION TRANSDUCERS

The most commonly used transducers for acoustic emission testing are broadband piezoelectric transducers. Although these transducers provide complete detection of the waveform, they have several drawbacks. There is a trade-off between sensitivity and bandwidth of this type of transducer. Background noises and the possibility of multiple cracks make it difficult to correlate waveforms to crack parameters. In addition, waveforms in the time domain might not be clear whether it occurs because of the source events or because of the specimen response as the test structure may also vibrate during the experiment. Kline et al.[11] suggested optical transducers to provide accurate and quantitative information, however this type of transducer is complex and expensive. Proctor[12] developed a high fidelity acoustic emission transducer using piezoelectric transduction. However, it is difficult to use this conical transducer in the field for long-term experiments. As acoustic emission propagates through the material, the AE event is distorted by dispersion, damping, mode conversion and reflections from boundaries[7]. These distortions may lead to erroneous location determination and inaccurate interpretation of test results, especially if broadband transducers are used. The other

transducer types, mostly used in the parametric studies of AE testing, are resonant type transducers. While these types of transducers have high sensitivity and are valuable for parametric studies, it is not possible to determine the frequency content of an AE event with a single transducer.

The MEMS chip reported here includes 10 different resonant type transducers located on 1 cm^2 area as explained above. We have shown using two simulation techniques that these transducers can be used to perform parametric studies. In addition, simultaneous output collection of multiple different resonant type transducers helps to compare how input signal frequency components and corresponding energies change. These outcomes show the possibility of not only the parametric study using a single commercial resonant type transducer, but also the information about the frequency content of the signal using all transducers simultaneously. Collecting various transducer outputs located very close to each other concurrently might make it possible to distinguish various mechanisms and various crack locations in the test body.

7. CONCLUSIONS

In this paper, the abilities of MEMS transducers developed for AE testing using two different acoustic emission simulation techniques were investigated. The essential idea is to develop a MEMS chip, which has the capabilities of resonant type and broadband type transducers. It is shown that the collection of multiple-resonant frequency transducers outputs simultaneously enables to accomplish the parametric study possibility of a single resonant transducer and to investigate the frequency nature of AE source event at the same time.

ACKNOWLEDGEMENTS

This material is based upon work supported by the National Science Foundation under Grant No. CMS-0329880, Pennsylvania Infrastructure Technology Alliance, and by Carnegie Mellon University and Lehigh University. The support from the sponsors is gratefully acknowledged. Any opinions, findings, and conclusions or recommendations expressed in this material are those of the authors and do not necessarily reflect the views of the sponsors.

REFERENCES

1. Ozevin, D., S.P. Pessiki, A. Jain, D.W. Greve, I.J. Oppenheim, “Development of a MEMS Device for Acoustic Emission Testing”, *Smart Structures and Materials 2003: Smart Systems and Nondestructive Evaluation for Civil Infrastructures*, San Diego, Proc. SPIE Vol. 5057, p. 64-74, March 2003.
2. Pardee, W.J., L.J. Graham, “Frequency Analysis of Two Types of Simulated Acoustic Emissions”, *Journal of the Acoustical Society of America*, March1978, p.793-799.
3. ASTM Standard E976-00.
4. Oppenheim, I.J., A. Jain, D.W. Greve, “Electrical Characterization of Coupled and Uncoupled MEMS Ultrasonic Transducers”, *IEEE Transactions on Ultrasonics, Ferroelectrics, and Frequency Control*, Vol.50, No.3, March2003, p.297-304.
5. Stephen, R.W.B., A.A. Pollock, “Waveforms and Frequency Spectra of Acoustic Emission”, *The Journal of the Acoustical Society of America*, Vol.50, 1971, p.904-910.
6. Goldsmith, W., *Impact*, Dover Publication, 1960, NY.
7. Hamstad, M.A., G.P. Sendeckyj, “Acoustic Emission Technology for Smart Structures”, *Journal of Acoustic Emission*, 1993, p.33-41.
8. Gaul, L., S. Hurlebaus, “Identification of The Impact Location on a Plate Using Wavelets”, *Mechanical Systems and Signal Processing*, Vol.12, 1997, p.783-795.
9. Kishimoto, K., H. Inoue, M. Hamada, T. Shibuya, “Time Frequency Analysis of Dispersive Waves by Means of Wavelet Transform”, *Journal of Applied Mechanics*, Vol.62, 1995, p.841-846.
10. Oppenheim, A.V., R.W. Schafer, J.R. Buck, *Discrete-Time Signal Processing*, 2nd Edition, 1999, Prentice Hall, NJ.
11. Kline, R.A., R.E. Green, C.H. Palmer, “A Comparison of Optically and Piezoelectrically Sensed Acoustic Emission Signals”, *Journal of the Acoustical Society of America*, Dec.1978, p.1633-1639.
12. Proctor, T.M., “Improved Piezoelectric Acoustic Emission Transducer”, *Journal of the Acoustical Society of America*, May1982, p.1163-1168.